

Forms of energy dissipated in the damaged zone of of underground cavities: Theoretical analysis and Finite Element Modeling

Hao Xu, Chloé Arson

School of Civil and Environmental Engineering, Georgia Institute of Technology, Atlanta, Georgia 30332, U.S.A.

Abstract

Keywords: Damage model, anisotropic, deviatoric stress, stress path, thermodynamic framework

e

1. Introduction

2. SoA on model of damage inducing irreversible deformation

2.1. damage and plasticity

The first work relating plasticity to damage is introduced by Lubliner [1] in concrete damage model, which defined the damage variable as the ratio of the dissipated plastic energy. In order to ensure the positivity of the damage variable within the framework of the Continuum Damage Mechanics, the damage potential is always proposed as the homogeneous function in terms of damage driving force. Due to the different constraints for the evolution of damage and irreversible strain, in general, the damage potential and the inelastic strain potential are chosen differently, which means the non-associated

flow rule is used in the model. The plasticity theory is coupled to a damage model to reflect the plastic (irreversible) deformation upon unloading [2, 3, 4]. $\mathbb{C}(\boldsymbol{\Omega}) + \epsilon^p$

2.2. extended CDM

Instead of coupling with the plasticity for permanent strain, the residual strain representing the crack opening after unloading can be taken into account by proposing a damage potential. [5, 6] Enriching the framework of CDM with microscopic properties of geomaterials is another strategy to account for the inelastic strain $\mathbb{C}(\boldsymbol{\Omega}) + \epsilon^{id}$

2.3. Multiscale strategy

The relationship between fracture mechanics and damage mechanics based on the thermodynamic considerations is built by Mazars & Pijaudier-Cabot [7]. This lead to the equivalent crack concept, in passing from a continuous damage zone to a discrete fracture. Distinct energy terms for the fundamental of cohesive method are studied by Gurtin, and he derived the energy release rate for a sharp crack surrounding by a homogeneous hyperelastic body.

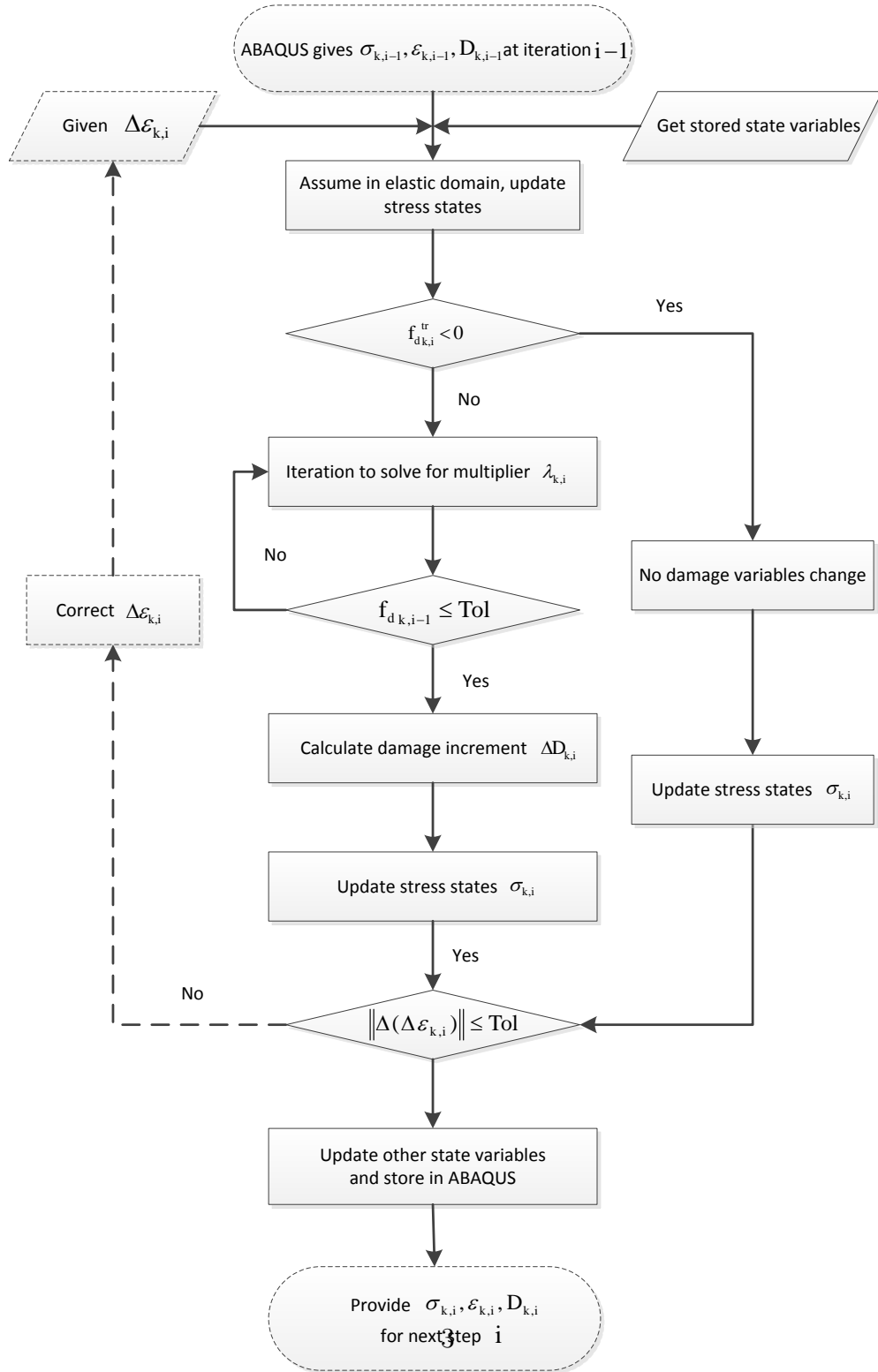


Figure 1: DSID model

2.4. *presentation of extended CDM approach (put equations of the model in appendix)*

2.5. *thermodynamic consistency*

3. Outline of the DSID model

3.1. *theoretical framework and algorithms*

3.2. *Numerical implementation (MATLAB, ABAQUS, residual)*

4. Element Level: analysis of the forms of energy dissipation

4.1. *Micro-scopic effects – Energy dissipation*

The Inequality of Clausius-Duhem is derived from the combination of the two first laws of thermodynamics:

$$\dot{\Phi}_s = \boldsymbol{\sigma} : \dot{\boldsymbol{\epsilon}} - \dot{\psi}_s \geq 0 \quad (1)$$

The free energy rate writes:

$$\dot{\psi}_s = \frac{\partial \psi_s}{\partial \boldsymbol{\epsilon}^E} : \dot{\boldsymbol{\epsilon}}^E + \frac{\partial \psi_s}{\partial \boldsymbol{\Omega}} : \dot{\boldsymbol{\Omega}} \quad (2)$$

The dissipation potential of solid skeleton should satisfy the Clausius-Duhem Inequality:

$$\dot{\Phi}_s = \boldsymbol{\sigma} : \dot{\boldsymbol{\epsilon}}^{id} + \mathbf{Y} : \dot{\boldsymbol{\Omega}} \geq 0 \quad (3)$$

The work by the external force is $\boldsymbol{\sigma} : \dot{\boldsymbol{\epsilon}}$ in each step, and $\dot{\Phi}_s$ is the dissipated energy during each load increment. The strain energy stored in the solid body is $\frac{1}{2} \boldsymbol{\sigma} : \boldsymbol{\epsilon}^E$. The energy lost in the loading should be always non-negative.

$$\boldsymbol{\sigma} : \dot{\boldsymbol{\epsilon}}^{id} + \mathbf{Y} : \dot{\boldsymbol{\Omega}} \geq 0 \quad (4)$$

4.1.1. Types of energy dissipation

The work by the external force is $\boldsymbol{\sigma} : \dot{\boldsymbol{\epsilon}}$ in each step, so the accumulate work is $\int \boldsymbol{\sigma} : \dot{\boldsymbol{\epsilon}} dt$. The accumulate strain energy stored in the solid body is $\frac{1}{2} \boldsymbol{\sigma} : \boldsymbol{\epsilon}^E$, and the dissipated energy is the differential between the the differential between external work and recoverable strain energy. The mechanical energy lost, $\int \dot{\Phi}_d dt$, in the loading is the area displayed in figure 2 with pink color and should be always non-negative, while the recoverable elastic strain energy is the area of the triangle as figure 2 with light green color.

$$\int \dot{\Phi}_d dt = \int \boldsymbol{\sigma} : \dot{\boldsymbol{\epsilon}} dt - \frac{1}{2} \boldsymbol{\sigma} : \boldsymbol{\epsilon}^E \geq 0 \quad (5)$$

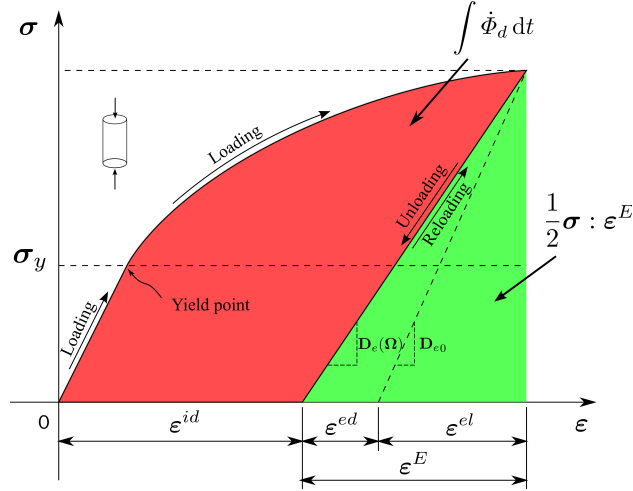


Figure 2: Energy spent in one loading process

The energy dissipated by damage is concluded into two means, crack generating without additional deformation and debonding paris of crack surfaces. Both of these two approaches can be represented by the mechanical response. Crack generation decrease the stiffness of material, which can increase the

capacity that material stores the energy; while debonding is related to non-linear strains. Since there are no other ways of energy transfer (thermal transport or radiation), the energy should be conserved in total. Based on response of material, all of the work by external loading should be splitted into three parts as figure 3 shows (The white part of energy is compensated by the extra part of the energy, related to irreversible strain, above the stress curve). It is also true from the strain decomposition in another side. The energy conservation is expressed as:

$$\int \boldsymbol{\sigma} : \dot{\boldsymbol{\epsilon}} dt = \int \boldsymbol{\sigma} : \dot{\boldsymbol{\epsilon}}^{el} dt + \int \boldsymbol{\sigma} : \dot{\boldsymbol{\epsilon}}^{ed} dt + \int \boldsymbol{\sigma} : \dot{\boldsymbol{\epsilon}}^{id} dt \quad (6)$$

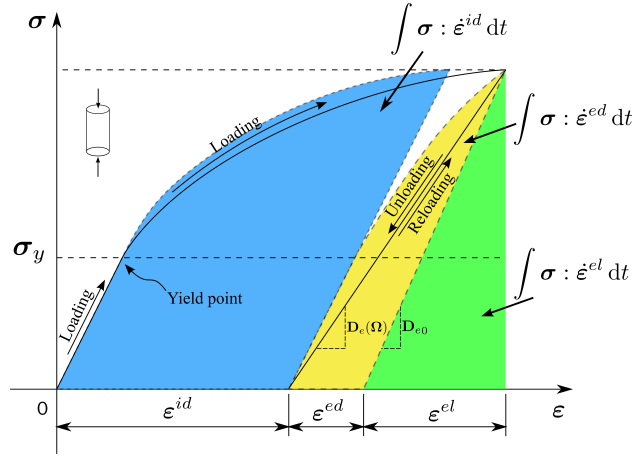


Figure 3: Energy splitting in one loading process

There are two parts of the energy related to elasto-damage strain, $\boldsymbol{\epsilon}^{ed}$. Not both of the elasto-damage strain is dissipated, some of them is stored in the solid body as strain energy ($\frac{1}{2} \boldsymbol{\sigma} : \dot{\boldsymbol{\epsilon}}^{ed}$); the other is dissipated (if material is unloaded), which won't induce the any strain increment. This part noted as

$\int \mathbf{Y} : \dot{\boldsymbol{\Omega}} dt$ is due to the crack generating but no displacement (figure 4).

$$\int \boldsymbol{\sigma} : \dot{\boldsymbol{\epsilon}}^{ed} dt = \frac{1}{2} \boldsymbol{\sigma} : \boldsymbol{\epsilon}^{ed} + \int \mathbf{Y} : \dot{\boldsymbol{\Omega}} dt \quad (7)$$

The energy related to debonding of the crack surfaces will be dissipated ($\int \boldsymbol{\sigma} : \dot{\boldsymbol{\epsilon}}^{id} dt$ related to irreversible strain) or stored ($\frac{1}{2} \boldsymbol{\sigma} : \dot{\boldsymbol{\epsilon}}^{ed}$, one part of energy related to elasto-damage strain.)

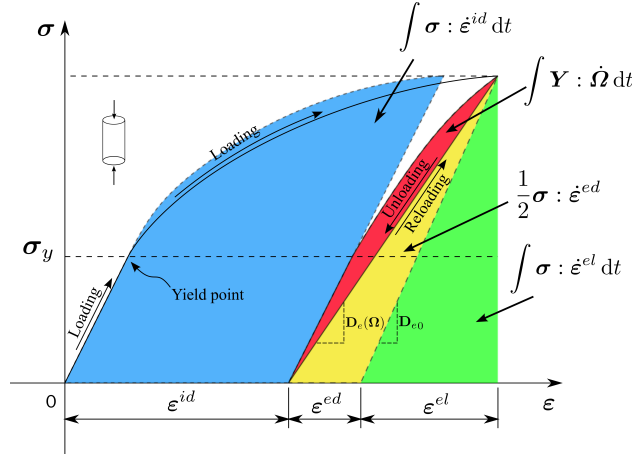


Figure 4: Energy splitting in one loading process

Based on the mechanical part, the lost of the energy is dissipated by the irreversible strain and crack generation due to damage.

$$\int \dot{\Phi}_d dt = \int \boldsymbol{\sigma} : \dot{\boldsymbol{\epsilon}}^{id} dt + \int \mathbf{Y} : \dot{\boldsymbol{\Omega}} dt \geq 0 \quad (8)$$

Therefore, the following equation is hold:

$$\int \boldsymbol{\sigma} : \dot{\boldsymbol{\epsilon}} dt - \frac{1}{2} \boldsymbol{\sigma} : \boldsymbol{\epsilon}^E = \int \boldsymbol{\sigma} : \dot{\boldsymbol{\epsilon}}^{id} dt + \int \mathbf{Y} : \dot{\boldsymbol{\Omega}} dt \quad (9)$$

If in the FEM, it could be written in the summation of all increments.

$$\sum \boldsymbol{\sigma}_{\theta n} : \dot{\boldsymbol{\epsilon}}_n - \frac{1}{2} \boldsymbol{\sigma}_n : \boldsymbol{\epsilon}_n^E = \sum \boldsymbol{\sigma}_{\theta n} : \dot{\boldsymbol{\epsilon}}_n^{id} + \sum \mathbf{Y}_{\theta n} : \dot{\boldsymbol{\Omega}}_n \quad (10)$$

Where $\sigma_{\theta n}$ and $Y_{\theta n}$ are the resultant stress and damage force during each increment when calculating the energy change:

$$\sigma_{\theta n} = (1 - \theta)\sigma_{n-1} + \theta \sigma_n \quad (11)$$

$$Y_{\theta n} = (1 - \theta)Y_{n-1} + \theta Y_n \quad (12)$$

θ is the approximation factor. The total elastic strain can be decomposed into:

$$\epsilon_n^E = \epsilon_{n-1}^E + \dot{\epsilon}_n^E = \epsilon_{n-1}^E + \dot{\epsilon}_n - \dot{\epsilon}_n^{id} \quad (13)$$

4.2. Limitations of the DSID Model

1. Meso-scopic effects

The “splitting effects” and “crossing effects” are considered in the DSID model. Both of them follow the Griffith criterion for the mode I failure in rocks. Therefore, the damage generated by pure shear stress and the damage induced by the equivalent principal stress are equal. The equivalence of these two status is lack of the microscopic effects to account for the difference between shear failure and tensile failure.

2. Micro-scopic effects

Indeedly, the DSID model does not include the failure mechanisms in micro-scale, but the crack debonding is captured by the damage model in terms of the energy. The splitting of the crack surfaces is the microscopic effect

4.3. Numerical Simulations of energy dissipation at element level

a few cases for 1 2 3, maps showing Φ dissipated W_e W_{ed}

E , ν (granite, shale, salt rock and claystone)

parametric study on the state of the rock (instead of stress)

Energy dissipation on different types of stress paths.

1. Uniaxial Tensile test

A uniaxial tensile test is computed with a 100 MPa pure shear stress in the REV.

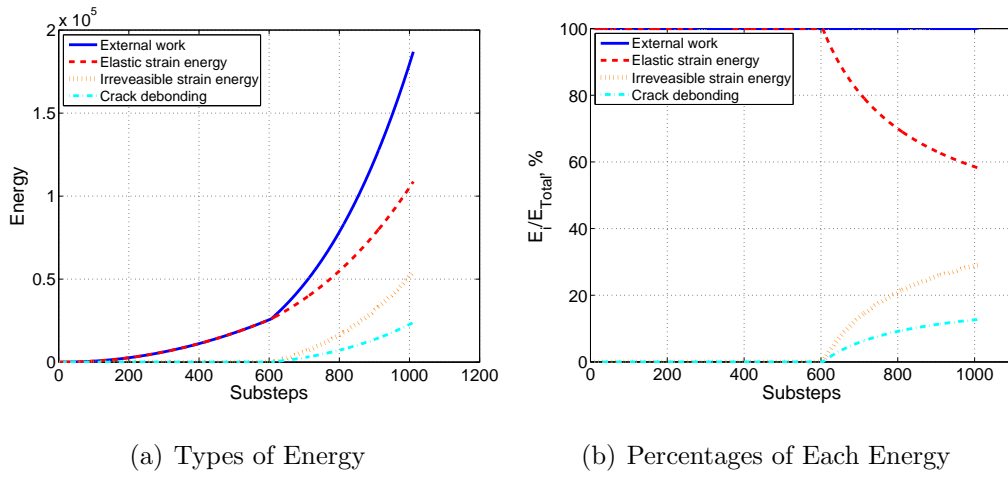


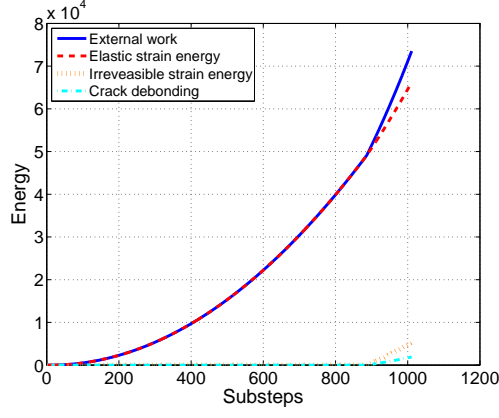
Figure 5: Energy in a uniaxial tensile test

2. Shear test

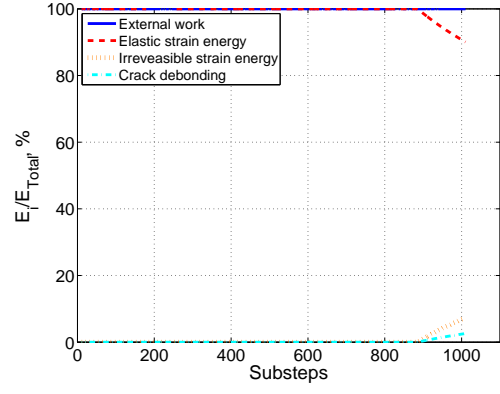
A pure shear test is simulated with $\sigma_{12} = 60$ MPa pure shear stress.

3. Triaxial Compression test

A triaxial compression test is computed with a 30 MPa confining stress and a vertical 130 MPa compressive stress. Each energy term in this simulation is summarized as follows.

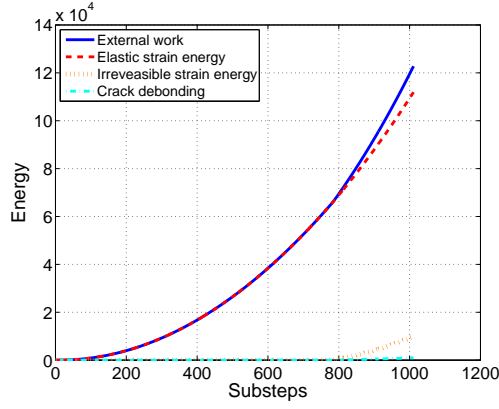


(a) Types of Energy

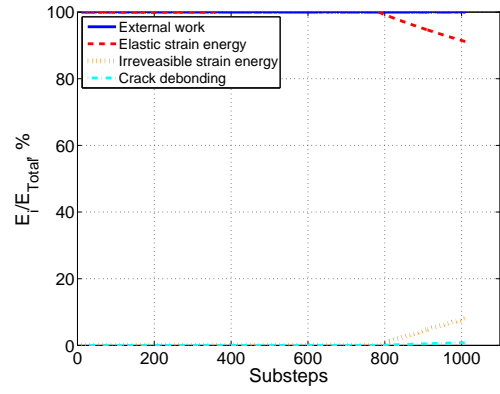


(b) Percentages of Each Energy

Figure 6: Energy in a shear test



(a) Types of Energy



(b) Percentages of Each Energy

Figure 7: Energy in a triaxial compression test

5. FEM simulation of damage dissipation driving propagation

5.1. Circular cavity

1. intact rock mass
2. with initial CDM damage
3. with initial notch

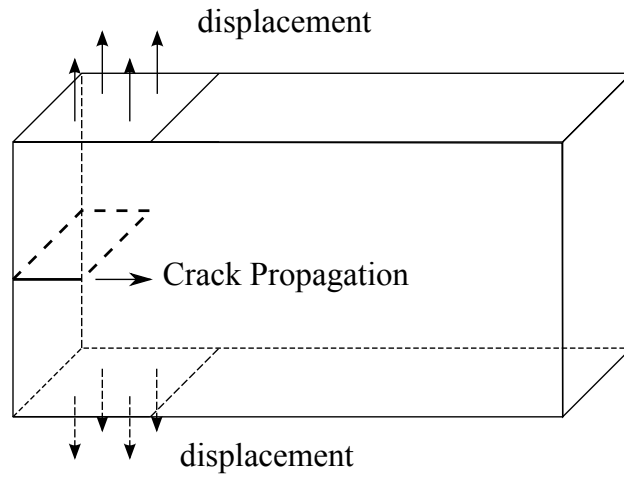


Figure 8: Sketch of the simulation problem

The dissipated energy in XFEM is:

$$\int \dot{\Phi}_d dt = \int G_c \dot{A} dt \quad (14)$$

If the dissipated energy in different methods is equivalent, the relation between these methods can be obtained.

$$\int \boldsymbol{\sigma} : \dot{\boldsymbol{\epsilon}}^{id} dt + \int \mathbf{Y} : \dot{\boldsymbol{\Omega}} dt = \int G_c \dot{A} dt \quad (15)$$

5.2. with complex crack patterns

5.3. Fracture patterns around cavities

6. Conclusion

Acknowledgments

This study was conducted at the Georgia Institute of Technology, as part of a research program on Finite Element Modeling of Hydraulic Fracturing. Funding was provided by ConocoPhillips, Houston, Texas.

Appendix A. The DSID Model

Appendix A.1. Outline of the DSID Model

For instance, [2] and [3] used a second-order damage tensor in a free energy potential expressed in terms of elastic strains, while [4] adopted the same approach with a different free energy expressed in terms of elastic strain and modified strains. However elastic strains cannot be controlled as such in an experiment or as a boundary condition in a numerical code. That is the reason why [5] and [6] expressed rock skeleton free energy in terms of total strains. Their model turned out to be easier to calibrate against experimental data. [8] and [9] employed a similar strategy, with the additional use of a parameter expressing the degree of anisotropy, allowing accounting for non-orthotropic damage. In uniaxial compression for instance, cracks can develop both parallel to the axis (orthotropic component of damage) and perpendicular to the axis (isotropic component of damage). An anisotropic damage model based on a stress-dependent free energy potential was proposed by [10]; [11], [12] and [13]. [13] used a modified stress tensor to account for the

difference between compressive and tensile stress. The damage evolution law derives from a criterion expressed in terms of the energy release rate conjugate to damage. In the former models on the contrary, damage evolution law is not derived from the damage potential with the energy release rate that is conjugate to damage: damage rate is calculated using associated variables used to predict crack lengths. Differences between the afore-mentioned damage models are highlighted in Table A.1.

Most anisotropic damage models for geomaterials postulate a skeleton free energy expressed in terms of deformation. As a result, the energy release rate \mathbf{Y} (also called damage driving force) conjugate to damage is also a function of deformation. In order to capture cracks due to “splitting effects” (i.e. Griffith cracks) and equivalent cracks due to “crossing effects” (i.e. wing shear cracks), it is necessary to make the damage criterion depend on a tensile damage driving force. In order to better account for states of tensile deformation under differential stress, the proposed anisotropic damage model is hyper-elastic, and a free energy potential expressed as a term of stress (Gibbs free energy, G_s) is proposed. This free energy accounts for the surface energy dissipated by opened cracks and closed cracks, and the elastic energy stored in material as well. To stay within the framework of linear elasticity in the absence of damage, the expression of the free energy should have at most quadratic terms of $\boldsymbol{\sigma}$ [5, 10] . The thermodynamic framework of the DSID model is summarized in Table. A.2. Stress/strain relationships are derived from the expression of a free energy potential. Damage evolution is controlled by a damage function, similar to Drucker-Prager yield function (but depending on the energy release rate). The damage flow rule is

Models	Free energy	Damage criterion or damage evolution law	Driving force	Stress	Vari-ables	Strain	Vari-ables
[2, 3]	$\psi_s(\boldsymbol{\varepsilon}^e, \boldsymbol{\phi}^\pm, \boldsymbol{\varepsilon}_{eq}^\pm, \boldsymbol{\phi}_{eq}^\pm)$ $= \psi^e(\boldsymbol{\varepsilon}^e, \boldsymbol{\phi}^\pm) + \Psi^p(\boldsymbol{\varepsilon}_{eq}^\pm) + \psi^d(\boldsymbol{\phi}_{eq}^\pm)$	$f_d^{\pm}(\mathbf{Y}^{\pm}, \phi_{eq}^{\pm})$	\mathbf{Y}^{\pm}	$\boldsymbol{\sigma}^{\pm}$		$\boldsymbol{\varepsilon}^e$ and $\boldsymbol{\varepsilon}_{eq}$	
[4]	$\psi_s = \psi^e(\boldsymbol{\varepsilon}^e, \boldsymbol{\Omega}) + \psi^d(\beta)$	$f_d(\mathbf{Y}, \beta)$	\mathbf{Y}			$\boldsymbol{\varepsilon}^e$ and $\bar{\boldsymbol{\varepsilon}}^e$	
[5, 6]	$\psi_s(\boldsymbol{\varepsilon}, \boldsymbol{\Omega})$	$f_d(\mathbf{Y}^+, \boldsymbol{\Omega})$	$\mathbf{Y}^+ = g\boldsymbol{\varepsilon}^+$			$\boldsymbol{\varepsilon}$ and $\boldsymbol{\varepsilon}^{\pm}$	
[8]	$\psi_s(\boldsymbol{\varepsilon}, d_i)$	$\mathbf{Q}^* = (1 - \xi)\mathbf{I} + \xi\boldsymbol{\Gamma}^*$ $\dot{\boldsymbol{\Omega}} = \mu\mathbf{Q}^*$	\mathbf{Y}			$\boldsymbol{\varepsilon}$	
[9]	$\psi_s(\boldsymbol{\varepsilon}^e, p, \boldsymbol{\Omega})$	$\dot{\boldsymbol{\Omega}} = \mathbb{S} : \mathbf{Y}$ $\mathbb{S} = (\beta - 1)\mathbb{I} + \mathbf{I} \otimes \mathbf{I}$	\mathbf{Y}	$\boldsymbol{\sigma}$ and effective stress $\hat{\boldsymbol{\sigma}}$		$\boldsymbol{\varepsilon}^e$	
[10, 11, 12]	$\psi_s(\boldsymbol{\sigma}, \boldsymbol{\Omega})$	based on micro-mechanics concepts	not included				
[13]	$\psi_s(\boldsymbol{\sigma}, r, \boldsymbol{\Omega}, \beta)$	$f_d(\mathbf{Y}, r, \boldsymbol{\Omega})$	\mathbf{Y}	$\boldsymbol{\sigma}$ and $\bar{\boldsymbol{\sigma}}$			

Table A.1: Comparison of Several Model Formulations for Anisotropic Damage.

non-associate, and the damage potential is chosen so as to ensure the positivity of dissipation associated to damage. The irreversible deformation due to damage follows an associated flow rule, which allows representing physical anisotropic trends of the deformation tensor during the damage process. More details are provided in [14].

- [1] J. Lubliner, J. Oliver, S. Oller, E. Onate, *International Journal of Solids and Structures* 23 (1989) 299–326.
- [2] R. K. Abu Al-Rub, S.-M. Kim, *Engineering Fracture Mechanics* 77 (2010) 1577–1603.
- [3] U. Cicekli, G. Z. Voyiadjis, R. K. Abu Al-Rub, *International Journal of Plasticity* 23 (2007) 1874–1900.
- [4] S. Murakami, K. Kamiya, *Int. J. Mech. Sci.* 39 (1996) 473–486.
- [5] D. Halm, A. Dragon, *Eur. J. Mech. A/ Solids* 17 (1998) 439–460.
- [6] F. Homand-Etienne, D. Hoxha, J. F. Shao, *Computers and Geotechnics* 22 (1998) 135–151.
- [7] J. Mazars, G. Pijaudier-Cabot, *International Journal of Solids and Structures* 33 (1996) 3327–3342.
- [8] J.-L. Chaboche, *International Journal of Damage Mechanics* 2 (1993) 311–329.
- [9] F. Pellet, A. Hajdu, F. Deleruyelle, F. Besnus, *Int. J. Numer. Anal. Meth. Geomech.* 29 (2005) 941–970.

Table A.2: Thermodynamic framework of the DSID model

D.S.I.D. Model		
Free Energy	$G_s(\boldsymbol{\sigma}, \boldsymbol{\Omega}) = \frac{1}{2} \boldsymbol{\sigma} : \mathbb{S}_0 : \boldsymbol{\sigma} + a_1 \text{Tr} \boldsymbol{\Omega} (\text{Tr} \boldsymbol{\sigma})^2 + a_2 \text{Tr}(\boldsymbol{\sigma} \cdot \boldsymbol{\sigma} \cdot \boldsymbol{\Omega})$ $+ a_3 \text{Tr} \boldsymbol{\sigma} \text{Tr}(\boldsymbol{\Omega} \cdot \boldsymbol{\sigma}) + a_4 \text{Tr} \boldsymbol{\Omega} \text{Tr}(\boldsymbol{\sigma} \cdot \boldsymbol{\sigma})$ $\boldsymbol{\varepsilon}^E = \frac{\partial G_s}{\partial \boldsymbol{\sigma}} = \frac{1 + \nu_0}{E_0} \boldsymbol{\sigma} - \frac{\nu_0}{E_0} (\text{Tr} \boldsymbol{\sigma}) \boldsymbol{\delta} + 2a_1 (\text{Tr} \boldsymbol{\Omega} \text{Tr} \boldsymbol{\sigma}) \boldsymbol{\delta} + a_2 (\boldsymbol{\sigma} \cdot \boldsymbol{\Omega} + \boldsymbol{\Omega} \cdot \boldsymbol{\sigma})$ $+ a_3 [\text{Tr}(\boldsymbol{\sigma} \cdot \boldsymbol{\Omega}) \boldsymbol{\delta} + (\text{Tr} \boldsymbol{\sigma}) \boldsymbol{\Omega}] + 2a_4 (\text{Tr} \boldsymbol{\Omega}) \boldsymbol{\sigma}$ $\mathbf{Y} = \frac{\partial G_s}{\partial \boldsymbol{\Omega}} = a_1 (\text{Tr} \boldsymbol{\sigma})^2 \boldsymbol{\delta} + a_2 \boldsymbol{\sigma} \cdot \boldsymbol{\sigma} + a_3 \text{Tr}(\boldsymbol{\sigma}) \boldsymbol{\sigma} + a_4 \text{Tr}(\boldsymbol{\sigma} \cdot \boldsymbol{\sigma}) \boldsymbol{\delta}$	
Damage Function	$f_d = \sqrt{J^*} - \alpha I^* - k$ $J^* = \frac{1}{2} (\mathbb{P}_1 : \mathbf{Y} - \frac{1}{3} I^* \boldsymbol{\delta}) : (\mathbb{P}_1 : \mathbf{Y} - \frac{1}{3} I^* \boldsymbol{\delta}), \quad I^* = (\mathbb{P}_1 : \mathbf{Y}) : \boldsymbol{\delta}$ $\mathbb{P}_1(\boldsymbol{\sigma}) = \sum_{p=1}^3 [H(\sigma^{(p)}) - H(-\sigma^{(p)})] \mathbf{n}^{(p)} \otimes \mathbf{n}^{(p)} \otimes \mathbf{n}^{(p)} \otimes \mathbf{n}^{(p)}$ $k = C_0 - C_1 \text{Tr}(\boldsymbol{\Omega})$	
Damage Potential	$g_d = \sqrt{\frac{1}{2} (\mathbb{P}_2 : \mathbf{Y}) : (\mathbb{P}_2 : \mathbf{Y})}$ $\mathbb{P}_2 = \sum_{p=1}^3 H[\max_{q=1}^3 (\sigma^{(q)}) - \sigma^{(p)}] \mathbf{n}^{(p)} \otimes \mathbf{n}^{(p)} \otimes \mathbf{n}^{(p)} \otimes \mathbf{n}^{(p)}$	
Flow Rule	$\dot{\boldsymbol{\varepsilon}}^{id} = \dot{\lambda}_d \frac{\partial f_d}{\partial \boldsymbol{\sigma}} = \dot{\lambda}_d \frac{\partial f_d}{\partial \mathbf{Y}} : \frac{\partial \mathbf{Y}}{\partial \boldsymbol{\sigma}}$ $\dot{\boldsymbol{\Omega}} = \dot{\lambda}_d \frac{\partial g_d}{\partial \mathbf{Y}}$	
G_s : Gibbs free energy	$\boldsymbol{\sigma}$: Stress tensor	$\boldsymbol{\Omega}$: Damage variable
$\boldsymbol{\varepsilon}^E$: Total elastic strain	ν_0 : Poisson's ratio	\mathbb{S}_0 : Undamaged compliance tensor
E_0 : Young's Modulus	$\boldsymbol{\delta}$: Kronecker delta	\mathbf{Y} : Damage driving force
f_d : Damage function	\mathbb{P}_1 and \mathbb{P}_2 : Projection tensors	$H(\cdot)$: Heaviside function
C_0 : Initial damage threshold	g_d : Damage potential	$\max(\cdot)$: Maximum function
$\dot{\boldsymbol{\varepsilon}}^{id}$: Irreavisable strain rate	$\dot{\lambda}_d$: Lagrangian Multiplier	$\dot{\boldsymbol{\Omega}}$: Damage rate
a_1, a_2, a_3, a_4 : Material parameters	$\sigma^{(p)}$ and $\mathbf{n}^{(p)}$: Principal stress and corresponding direction	C_1 : Damage hardening variable

- [10] J. Shao, H. Zhou, K. Chau, International Journal for Numerical and Analytical Methods i Geomechanics 29 (2005) 1231 – 1247.
- [11] J. F. Shao, K. T. Chau, X. T. Feng, International Journal of Rock Mechanics & Mining Sciences 43 (2006) 582–592.
- [12] J. Zhou, J. Shao, W. Xu, Mechanics Research Communications 33 (2006) 450–459.
- [13] K. Hayakawa, S. Murakami, International Journal of Damage Mechanics 6 (1997) 333–363.
- [14] H. Xu, C. Arson, International Journal of Computational Methods, Special Issue on Computational Geomechanics 11 (2014).